Free Radical Biology & Medicine 48 (2010) 411–420

Contents lists available at ScienceDirect

Free Radical Biology & Medicine

journal homepage: www.elsevier.com/locate/freeradbiomed

Original Contribution

Yeast frataxin mutants display decreased superoxide dismutase activity crucial to promote protein oxidative damage

Verónica Irazusta, Elia Obis, Armando Moreno-Cermeño, Elisa Cabiscol, Joaquim Ros *, Jordi Tamarit

Grup de Bioquímica de l'Estrés Oxidatiu, Departament de Ciències Mèdiques Bàsiques, Facultat de Medicina, Universitat de Lleida, 25008 Lleida, Spain

ARTICLE INFO

Article history:
Received 26 June 2009
Revised 25 October 2009
Accepted 16 November 2009
Available online 8 December 2009

Keywords:
Iron overload
Protein carbonylation
Metal-catalyzed oxidation
Frataxin
Yeast
Superoxide dismutase
Iron toxicity
Friedreich ataxia
Free radicals

ABSTRACT

Iron overload is involved in several pathological conditions, including Friedreich ataxia, a disease caused by decreased expression of the mitochondrial protein frataxin. In a previous study, we identified 14 proteins selectively oxidized in yeast cells lacking Yfh1, the yeast frataxin homolog. Most of these were magnesium-binding proteins. Decreased Mn-SOD activity, oxidative damage to CuZn-SOD, and increased levels of chelatable iron were also observed in this model. This study explores the relationship between low SOD activity, the presence of chelatable iron, and protein damage. We observed that addition of copper and manganese to the culture medium restored SOD activity and prevented both oxidative damage and inactivation of magnesium-binding proteins. This protection was compartment specific: recovery of mitochondrial enzymes required the addition of manganese, whereas cytosolic enzymes were recovered by adding copper. Copper treatment also decreased Δ*yfh1* sensitivity to menadione. Finally, a Δ*sod1* mutant showed high levels of chelatable iron and inactivation of magnesium-binding enzymes. These results suggest that reduced superoxide dismutase activity contributes to the toxic effects of iron overloading. This would also apply to pathologies involving iron accumulation.

Iron plays an essential role in cellular metabolism due to its great versatility as a biological catalyst [1]. However, high tissue iron concentrations have been associated with the development and progression of several pathological conditions [2], including genetic disorders caused by mutations in proteins directly involved in iron metabolism, such as hereditary hemochromatosis, Friedreich ataxia (FRDA), aceruloplasminemia, and X-linked sideroblastic anemia [3]. Increased body iron stores that could contribute to pathology progression have been described in other disorders, such as cancer [4] and Parkinson disease [5].

FRDA is caused by decreased expression of the mitochondrial protein frataxin [6]. Many studies have linked frataxin to iron metabolism and iron overload. Consequently, some therapeutic approaches under study seek to reduce the degree of iron accumulation using chelators [7] or siderophores or to prevent its pro-oxidant effects with antioxidants such as idebenone, a coenzyme Q analog [8]. In most cellular and animal models of FRDA, decreased activity of proteins containing iron–sulfur clusters has been reported, suggesting that frataxin has a role in iron–sulfur cluster biosynthesis [9]. However, the precise function of this protein remains a matter of debate. Many studies of frataxin function have used *Saccharomyces cerevisiae,* as frataxin and the yeast homolog Yfh1 are orthologs. Frataxin and Yfh1 are mitochondrial proteins, Δ*yfh1* strains accumulate iron and show decreased activity of iron–sulfur-containing proteins [10], and human frataxin complements yeast Δ*yfh1* mutant strains [11].

Iron toxicity is related to its ability to trigger the generation of reactive oxygen species (ROS) [12]. These species are highly reactive and have the potential to damage cellular components such as lipids, nucleic acids, carbohydrates, and proteins. "Free iron" is considered to be the iron fraction that is in transit between uptake and release from iron-binding proteins and is directly involved in iron toxicity. Although the exact nature of this iron fraction, also termed "chelatable iron," "redox-active iron," or "labile iron pool" [13], is poorly defined, it is generally considered to be associated with small-molecular-weight ligands such as ATP, ADP, phosphate, or citrate [1,14]. All living organisms have developed iron transport and storage systems that keep concentrations of free iron as low as possible [13].

In a previous study, we addressed the consequences of iron overload on the cellular proteome of a yeast model of Friedreich ataxia [15]. By analyzing protein carbonylation, one of the end-products of free radical attack on proteins, we identified 14 proteins specifically carbonylated in Δ*yfh1* mutants. Most of these were Mg-binding proteins, indicating that iron can replace Mg-binding sites and specifically promote damage of this group of proteins. Our results also indicated that chelatable iron, and not total cellular iron, was the iron fraction directly involved in promoting protein damage.

Our proteomic search for iron targets in Δ*yfh1* mutants also identified the cytosolic CuZn-dependent superoxide dismutase (SOD1) as one of the damaged enzymes [15]. Independent results from our lab [16] and others [17] have shown that iron overload in

* Corresponding author. Fax: +34 973 702 426.
E-mail address: joaquim.ros@cmb.udl.es (J. Ros).

0891-5849/$ – see front matter © 2009 Elsevier Inc. All rights reserved.
doi:10.1016/j.freeradbiomed.2009.11.010

yeast promotes inactivation of SOD2, and a similar effect was recently reported in a mouse model of hereditary hemochromatosis [18]. These data suggest that, in addition to its known catalytic ability to generate reactive oxygen species, iron overload could promote oxidative stress by inactivating both the mitochondrial and the cytosolic superoxide dismutases. This study shows that decreased SOD activity promotes increased levels of chelatable iron, which in turn promote specific protein damage in a yeast model of FRDA.

Experimental procedures

Organisms and culture conditions

The *S. cerevisiae* strains used in this work were W303-1A (wild type; MATa *ura3-52 leu2-3,112 trp1-1 his3-11,15 ade2-1*) and its isogenic null mutants MML298 (Δ*yfh1;* MATa *yfh1::kanMX4*) [15,16], BQS102 (Δ*sod1;* MATa *sod1::URA3*), and BQS050 (Δ*yfh1*Δ*sod1;* MATa *yfh1::kanMX4, sod1::URA3*). BQS050 and BQS102 were obtained by replacing the SOD1 open reading frame in either W303-1A or MML298 with a *URA3* cassette obtained by PCR amplification from strain 96687 (MATa *sod1::URA3;* American Type Culture Collection, Manassas, VA, USA). Yeast cells were grown in rich medium (1% yeast extract, 2% peptone) with either 2% glucose (YPD) or 3% glycerol (YPG) by incubation in a rotary shaker at 30°C. Synthetic medium (SC) contained 2% glucose, 0.67% yeast nitrogen base (Difco), a mixture of amino acids, and the required auxotrophic supplements. All experiments were performed with exponentially growing cells at optical densities ranging from 0.5 to 1 ($\lambda = 600$ nm, 1-cm light path).

Two-dimensional gel electrophoresis

Cells were suspended in 25 mM Tris–HCl buffer, pH 8, plus 8 M urea and disrupted using glass beads. An equal volume of 8 M urea, 8% Chaps, and 50 mM dithiothreitol (DTT) was added to the lysed cells, and after centrifugation (12,000 rpm for 10 min) protein amounts in the supernatant were quantitated with a Nanodrop ND-100 spectrophotometer and 40 μg of protein was diluted in 150 μl of rehydration buffer (8 M urea, 4% Chaps, 25 mM DTT, 0.5% Bio-Lytes). Isoelectric focusing was performed in 7-cm IPG immobilized pH gradient strips (3-10 NL Bio-Rad). After the first dimension, the strips were incubated for 20 min with 5 ml of a solution containing 10 mM 2,4-dinitrophenylhydrazine (DNPH) in 10% trifluoroacetic acid. DNPH reacts with carbonyl groups in proteins. Antibodies against DNPH allow immunodetection of this compound bound to carbonyl groups in proteins by classic Western blot techniques. To stop this reaction, the strips were transferred to a 5-ml solution containing 0.4 M Tris, pH 8.8, 6 M urea, 2% SDS, and 20% glycerol. Second-dimension SDS–PAGE was performed on 18×18-cm 12.5% polyacrylamide gels. For comparative purposes, two strips (one corresponding to wild-type cells and the other to Δ*yfh1* cells grown under the same conditions) were run in parallel on the same gel to obtain images with the same exposure and incubation times. Gels were either transferred to PVDF membranes for Western blot analysis or silver stained (PlusOne silver staining kit; General Electric Healthcare) and scanned in a GS800 densitometer (Bio-Rad). Antibodies against DNPH (Dako) were used at 1:5000 dilution. A peroxidase-conjugated anti-rabbit antibody was used for detection. Images were acquired in a ChemiDoc XRS System (Bio-Rad) and analyzed with PDQuest software (Bio-Rad).

Enzyme activity

Cell extracts were prepared using glass beads, and enzymatic activity was assayed as previously described for aconitase and succinate dehydrogenase [19], pyruvate kinase [20], and phosphoglycerate kinase [21]. Mitochondrial F_1F_0 ATP synthase was assayed in mitochondrial preparations as described [22]. Oligomycin at 6 μg/ml, an inhibitor of this enzyme [23], was used for background subtraction. Mitochondria were prepared as described [19]. Superoxide dismutase activity was analyzed in zymograms. Briefly, cells were disrupted using glass beads in 50 mM Tris–HCl buffer, pH 8.0. Crude extracts were loaded onto native 12% Tris–glycine polyacrylamide gels, pH 8.8. After electrophoresis, gels were stained for SOD activity as described [24]. Native gels were subjected to densitometry and the density of the bands corresponding to Mn-SOD or CuZn-SOD activity was calculated using Quantity One software (Bio-Rad).

Iron analyses

Total cellular iron was determined in nitric acid-digested cells, using bathophenanthroline sulfonate as chelator [25]. Intracellular chelatable iron was determined using confocal microscopy and the fluorescent iron chelator Phen Green SK diacetate (Molecular Probes) [15]. Yeast cells were grown in YPD medium, washed twice with SC medium, and then loaded for 20 min with 20 μM Phen Green SK diacetate in 300 μl of SC medium. This incubation was performed over glass coverslips treated with concanavalin A (Sigma) to fix the cells and mounted in a stainless steel chamber placed on the stage of an inverted Olympus FV500 confocal laser scanning microscope. After 20 min incubation with Phen Green SK diacetate, the cells fixed on the chamber's coverslip were washed twice with SC medium, diluted again in 300 μl of SC medium, and imaged in the microscope using an argon laser ($\lambda_{excitation}$ 488 nm), 505 nm longpass filter, and Olympus PlanApo oil objective (60×/1.40 NA). For dynamic measurements of Phen green dequenching, images were collected at 5-s intervals. After 1 min, 3 μl of a solution containing 0.2 M 1,10-phenanthroline was added to the chamber and images were collected for 4 additional minutes at 5-s intervals. Data were analyzed using Olympus Fluoview and Microsoft Excel software.

Measurement of cell growth rate

Cell growth was monitored in 1-ml cultures in 24-well plates incubated at 30°C and constant agitation in a Biotek PowerWave XS microplate spectrophotometer. Plates were sealed with Breathe Easy membranes (Diversified Biotech, Boston, MA, USA). Optical density (600 nm) was recorded every 30 min. Generation times were calculated using Gen5 data analysis software and Microsoft Excel.

Results

CuZn-SOD activity is decreased in Δyfh1 cells

In two previous proteomic analyses of Δ*yfh1* yeast cells, we identified CuZn-superoxide dismutase as both a highly induced protein [16] and a target of iron-induced oxidative stress [15]. The degree of carbonylation significantly exceeded the increase in SOD1 protein, suggesting that a fraction of this protein may be present in a damaged form in Δ*yfh1* cells. However, the consequences of such carbonylation on SOD1 activity were not studied. To reveal whether total SOD1 activity was altered in Δ*yfh1* cells, this study analyzed the activity of both SOD isoenzymes using native gels stained for SOD activity. As shown in Figs. 1A and 1B, CuZn-SOD activity was slightly decreased in Δ*yfh1*. The SOD1 activity decrease appears stronger when specific activity (Fig. 1C) is calculated by dividing the enzymatic activity with the protein amounts measured by Western blot (Fig. 1A). The origin of such low specific activity may be protein carbonylation due to ROS damage but could also be related to limited copper availability, which would result in large amounts of apo-SOD1 protein. This is very possible, as copper is required for the activity of Fet3, a multicopper oxidase involved in iron transport that is largely induced in Δ*yfh1* strains [26]. Indeed, it has been described that activation of iron acquisition by the iron-responding factor Aft1 increases copper

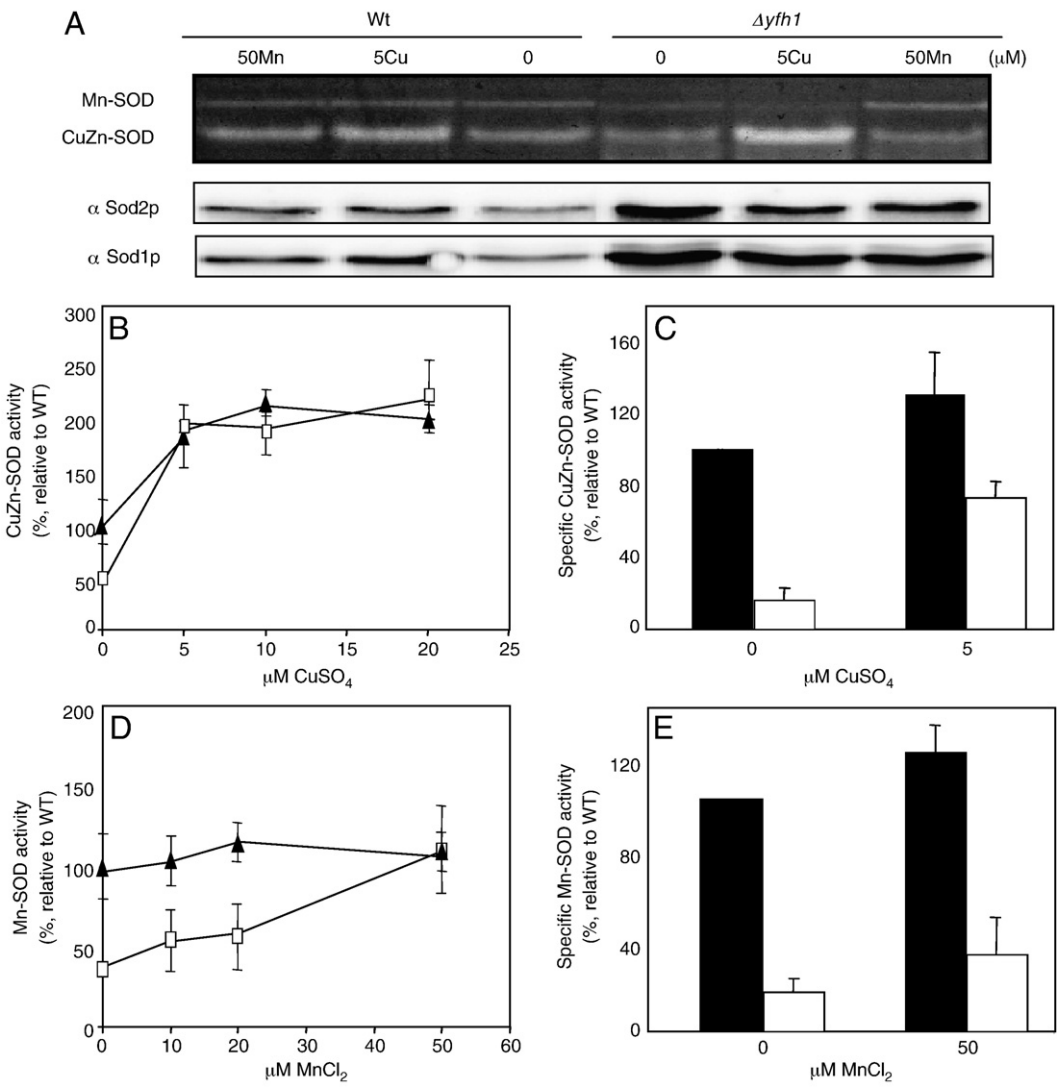

Fig. 1. SOD activity in Δ*yfh1* cells. Crude extracts from wild-type and Δ*yfh1* cells grown under various conditions were loaded on native gels and SOD activity was detected as explained under Experimental procedures. Crude extracts were also separated by SDS–PAGE and the amounts of SOD1 and SOD2 calculated by Western blot. (A) Zymograms and Western blots showing the activity and amounts of both isoenzymes in crude extracts from cells grown in YPG supplemented or not with 5 μM $CuSO_4$, 50 μM $MnCl_2$. (B) Total CuZn-SOD activity in cells grown in supplemented YPG medium was calculated by analyzing the intensity of the corresponding band in the zymogram. Activity in nonsupplemented wild-type cells was considered the 100% reference value. (C) Specific CuZn-SOD activity was calculated by dividing the relative enzymatic activity (obtained by zymograms) by the relative intensity of the Western blot bands against SOD1. Activity in nonsupplemented wild-type cells was considered the 100% reference value. (D and E) In manganese-supplemented cultures, total and specific Mn-SOD activity was calculated as explained for CuZn-SOD. All data are presented as means ± standard deviation of three independent experiments.

transport into membrane compartments, leading to copper-deprived cytosol [27]. To investigate whether copper availability may be limited in Δ*yfh1* cells, we supplemented the culture medium with copper sulfate at various concentrations. As shown in Fig. 1B, copper treatment increased CuZn-SOD activity in both wild-type and Δ*yfh1* cells. In wild-type cells, this was due to higher protein expression, as observed by Western blot (Fig. 1A). Consequently, specific activity was not altered (Fig. 1C). Recovery of wild-type levels of CuZn-SOD activity in Δ*yfh1* cells was achieved with 5 μM concentration of $CuSO_4$. Supplementing culture medium with higher concentrations of copper did not further increase SOD activity. However, specific activity was not fully restored. This fact may indicate that, in addition to limited copper availability, a fraction of CuZn-SOD may be inactive in Δ*yfh1* cells because of oxidative damage.

We also investigated the effects of copper and manganese treatment on Mn-SOD activity. In a previous study [16], we observed that the mitochondrial manganese-dependent isoenzyme (Mn-SOD) showed a marked increase in protein amounts, but paradoxically decreased activity in Δ*yfh1* cells. This decreased activity was considered one of the consequences of the manganese deficiency found in Δ*yfh1* cells and could be reverted by manganese supplementation of the culture medium. The zymograms shown in Fig. 1A confirmed this marked decrease in Mn-SOD activity in Δ*yfh1* cells and its recovery by manganese (Fig. 1D). However, when specific activity was calculated, large amounts of inactive SOD2 were present, even in manganese-supplemented cultures (Fig. 1E). This fact indicates that Mn-SOD may be inactivated by iron accumulation in mitochondria, as well as by manganese deficiency. Iron would occupy the active site of the enzyme [17], yielding an inactive and easily oxidizable [15] form of this enzyme.

Carbonyl content in supplemented cultures

In a previous study, we used a proteomics approach to identify oxidatively damaged proteins in a Δ*yfh1* strain. This approach consisted of Western blot detection of carbonyl groups on proteins previously separated by two-dimensional gel electrophoresis (2D-oxy blot). We identified 17 spots with increased carbonyl content in Δ*yfh1*

cells, corresponding to 14 different proteins. To explore the contribution of decreased SOD activity to the carbonylation of this group of proteins, we analyzed protein carbonylation in yeast cells grown in YPG medium supplemented or not with 50 μM $MnCl_2$ and 5 μM $CuSO_4$. As shown in Fig. 1, recovery of wild-type levels of CuZn-SOD and Mn-SOD in Δ*yfh1* cells was achieved with these metal concentrations. Crude extracts were prepared and analyzed by 2D-oxy blots as described under Experimental procedures. Replicate gels were silver stained to measure the changes in protein amounts of every analyzed spot under each experimental condition. Representative images of these gels are shown in Fig. 2. Both 2D-oxy blots and silver-stained gels were analyzed in pairs (wild type vs Δ*yfh1*) using PDQuest software. Relative carbonyl and protein amounts (Δ*yfh1*/wild type) obtained for each spot are shown in Table 1. These results are summarized in Fig. 3, which presents the increase in carbonylation in Δ*yfh1* cells of each protein analyzed (corrected considering changes in protein amounts), in treated and untreated cultures. A significant decrease in the carbonylation degree of most of the analyzed proteins was observed after manganese and copper treatment. As a control, spot 18, which showed no change in carbonylation in Δ*yfh1* cells, was identified as the two isoforms of glyceraldehyde-3P dehydrogenase (TDH2 and TDH3). Previously, we had shown that glyceraldehyde-3P dehydrogenase activity was not altered in Δ*yfh1* mutants [15]. As shown in Fig. 3, metal treatment had no effect on the degree of carbonylation, suggesting that these proteins are damaged as a consequence of increased superoxide levels produced in Δ*yfh1* cells.

Recovery of enzymatic activity by copper and manganese treatments

To validate the results obtained in the previous experiments, we analyzed the enzymatic activity of pyruvate kinase, phosphoglycerate kinase, and mitochondrial ATP synthase in YPG cultures supplemented or not with copper and manganese. These three enzymes were described as targets of iron-induced oxidative stress in Δ*yfh1* cells because their enzymatic activities decreased and carbonyl content increased in such cells [15]. Fig. 4 shows that manganese and copper treatment protected these enzymatic activities from inactivation in Δ*yfh1* cells, confirming the proteomic data presented in Table 1 and Fig. 3. We also wanted to determine if copper alone was able to recover both cytosolic and mitochondrial enzymes; a cross-compartment protection by CuZn-SOD of mitochondrial enzymes such as homoaconitase or aconitase has been reported [28]. Only the cytosolic proteins pyruvate kinase and phosphoglycerate kinase were recovered by copper treatment, whereas recovery of the mitochondrial ATP synthase required both copper and manganese. This result suggests that these enzymes are inactivated as a consequence of increased

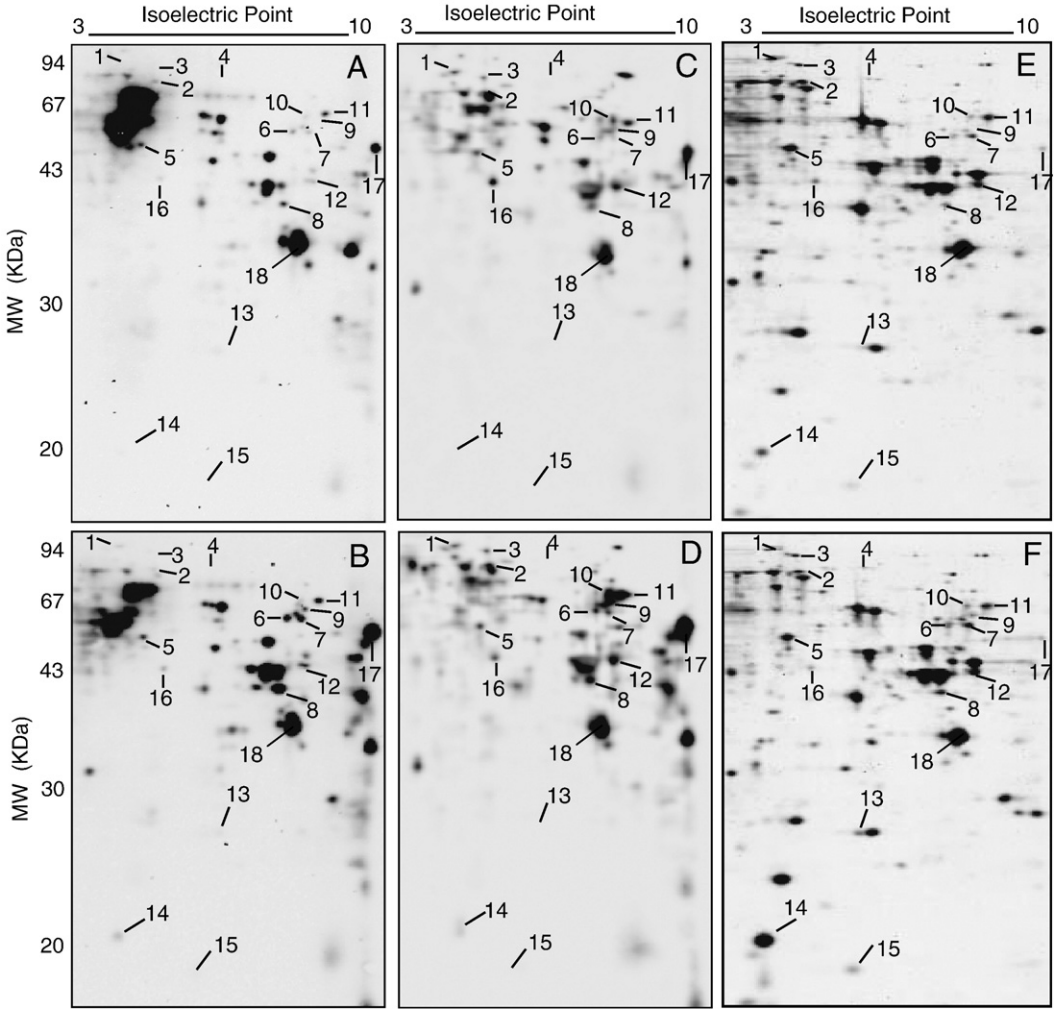

Fig. 2. Analysis of the oxyproteome of wild-type and Δ*yfh1* cells grown in metal-supplemented YPG by two-dimensional gel electrophoresis. Cells were grown in YPG medium supplemented with 50 μM $MnCl_2$ and 5 μM $CuSO_4$ as indicated. Control cultures were grown without supplementation. Cell lysates (40 μg of total protein) were separated by two-dimensional gel electrophoresis as described under Experimental procedures. Gels were transferred to PVDF membranes and oxidized proteins detected with antibodies against 2,4-dinitrophenol: (A) wild-type and (B) Δ*yfh1* cells grown in unsupplemented YPG; (C) wild-type and (D) Δ*yfh1* cells grown in supplemented YPG. (E and F) Silver-stained gels correspond to (E) wild-type and (F) Δ*yfh1* cells grown in supplemented YPG. The indicated spots are those previously identified as targets of oxidative stress in Δ*yfh1* cells [15] (see Table 1).

Table 1
Analysis of specific protein carbonylation in Δ*yfh1* cells grown in YPG medium supplemented or not with copper and manganese

Protein	Gene	Spot	Untreated			5 μM $CuSO_4$ + 50 μM $MnCl_2$		
			Oxidation increase	Protein increase	Oxidation/protein	Protein increase	Protein increase	Oxidation/protein
Mitochondrial heat shock protein	*SSC1*	1	3.43 ± 1.74	0.86 ± 0.46	4.0 ± 0.6	1.17 ± 0.33	0.62 ± 0.47	2.34 ± 0.90
		3	3.27 ± 0.41	1.19 ± 0.60	2.75 ± 0.83	1.68 ± 0.42	0.74 ± 0.20	2.25 ± 0.014
Mitochondrial matrix chaperone	*HSP78*	4	14.47 ± 1.15	0.92 ± 0.25	15.75 ± 3.0	2.19 ± 0.35	1.35 ± 0.65	1.62 ± 0.81
Cytoplasmic heat shock protein homolog	*SSE1*	2	6.61 ± 3.48	0.96 ± 0.29	6.8 ± 2.1	2.27 ± 0.01	0.74 ± 0.36	3.027 ± 1.39
F_1F_0 ATP synthase, α subunit	*ATP1*	6	5.47 ± 0.60	1.21 ± 0.20	4.6 ± 0.28	1.56 ± 0.79	1.98 ± 0.92	0.79 ± 0.15
		7	12.62 ± 3.45	1.00 ± 0.30	12.69 ± 0.4	1.72 ± 0.82	1.64 ± 0.42	1.04 ± 0.17
F_1F_0 ATP synthase, β subunit	*ATP2*	5	3.43 ± 1.25	0.67 ± 0.38	5.30 ± 1.7	1.43 ± 0.67	0.71 ± 0.25	2.05 ± 0.91
Acetohydroxy acid reductoisomerase	*ILV5*	8	10.20 ± 2.41	0.98 ± 0.55	10.4 ± 2.9	1.02 ± 0.54	1.83 ± 0.87	0.49 ± 0.13
Pyruvate kinase 1	*CDC19*	10	3.60 ± 1.25	0.90 ± 0.10	3.90 ± 1.01	1.02 ± 1.42	1.63 ± 1.2	0.61 ± 0.55
		11	2.73 ± 0.55	0.80 ± 0.20	3.5 ± 0.19	1.65 ± 0.06	1.34 ± 0.51	1.15 ± 0.43
3-Phosphoglycerate kinase	*PGK1*	12	4.00 ± 0.75	1.02 ± 0.25	3.9 ± 0.27	1.71 ± 0.51	0.93 ± 0.51	1.85 ± 0.45
Adenylate kinase	*ADK1*	13	8.30 ± 1.35	2.50 ± 0.53	3.3 ± 0.21	1.71 ± 0.51	3.17 ± 0.92	0.54 ± 0.02
Catalase A	*CTA1*	9	49.37 ± 5.75	6.07 ± 1.74	8.46 ± 2.8	2.17 ± 0.86	7.13 ± 5.30	0.35 ± 0.13
Thiol-specific peroxiredoxin	*AHP1*	14	15.33 ± 4.43	4.37 ± 1.07	3.50 ± 0.73	6.76 ± 2.31	6.53 ± 0.92	1.03 ± 0.27
CuZn-superoxide dismutase	*SOD1*	15	14.83 ± 2.84	5.01 ± 2.03	2.97 ± 0.74	5.20 ± 1.44	2.11 ± 0.38	2.44 ± 0.27
Actin, α chain	*ACT1*	16	2.63 ± 0.25	0.77 ± 0.06	3.43 ± 0.19	1.24 ± 0.50	0.55 ± 0.17	2.22 ± 0.37
Translational elongation factor EF-1α	*TEF2*	17	9.20 ± 1.45	1.24 ± 0.42	7.51 ± 1.41	1.87 ± 0.73	0.82 ± 0.07	2.28 ± 0.53
Glyceraldehyde-3-phosphate dehydrogenase	*TDH2/3*	18	0.94 ± 0.11	0.89 ± 0.41	1.06 ± 0.28	0.95 ± 0.49	0.85 ± 0.02	1.12 ± 0.56

The spots indicated in Fig. 2 were previously identified as the indicated proteins [15]. Oxidation increase (Δ*yfh1* over wild type) was quantified from the oxy blots shown in Fig. 2. Protein increase (Δ*yfh1* over wild type) was quantified from silver-stained gels. Values in the last column are the ratio between oxidation and protein increases and represent the relative increase in oxidative damage for each protein in Δ*yfh1*. Data are mean ± confidence intervals (α = 0.05) from four independent experiments.

superoxide levels found in Δ*yfh1* cells in their respective cellular compartments. To further investigate the contribution of CuZn-SOD activity to the inactivation of mitochondrial enzymes in Δ*yfh1* cells, we analyzed the effects of copper alone or in conjunction with manganese on the activity of two representative iron–sulfur enzymes, aconitase and succinate dehydrogenase. In a previous study, we showed that inactivation of several iron–sulfur enzymes, one of the hallmarks of FRDA, could be prevented in Δ*yfh1* cells when Mn-SOD was recovered by manganese treatment [16]. The exception was aconitase, which still presented low levels of activity after manganese treatment. As shown in Fig. 5, copper alone had no effect on aconitase and succinate dehydrogenase activity. The combined treatment (copper plus manganese) restored succinate dehydrogenase activity, but had no effect on aconitase activity. These results confirm our previous observation that aconitase is more dependent on the presence of Yfh1 than other iron–sulfur enzymes and also that decreased CuZn-SOD activity in Δ*yfh1* cells has little effect on mitochondrial enzymes.

Effects of copper and manganese treatments on cell growth rate and sensitivity to menadione

When grown in YPG, Δ*yfh1* cells present a decrease in cell growth rate. Because copper and manganese prevented protein damage in Δ*yfh1* cells, we investigated the effects of such supplementation on cell growth rate. To test several combinations of both metal concentrations and to detect slight changes in growth rate, we performed these experiments in liquid media in multiwell plates.

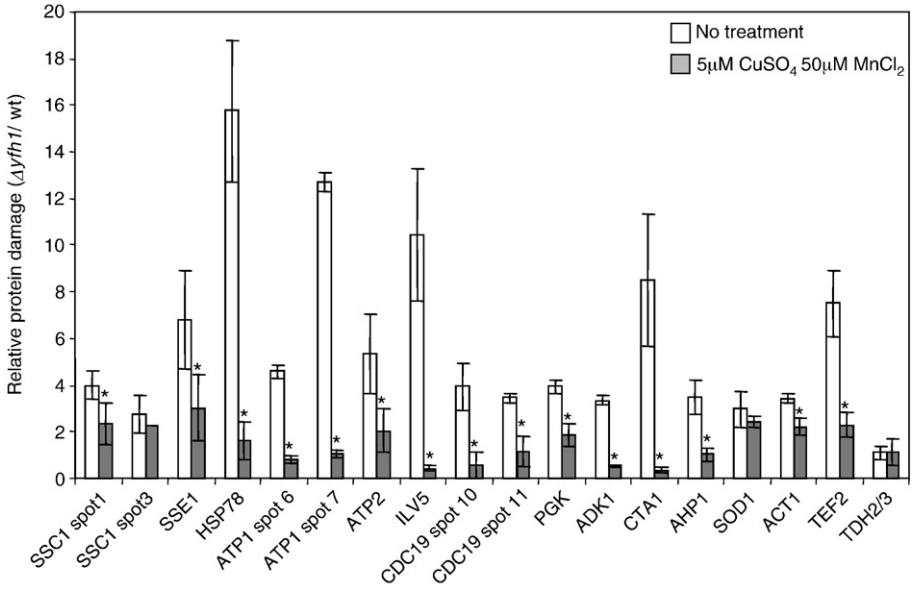

Fig. 3. Comparative analysis of specific protein damage in untreated and treated cultures. Values are the ratios between the changes observed in protein carbonylation (by oxy-blots) and the protein amounts (silver-stained gels) for each specific spot and represent the relative increase in oxidative damage in Δ*yfh1* for each protein analyzed under the various growth conditions. Error bars represent confidence intervals (α = 0.05). *Significant decrease in the relative protein damage value after metal treatment.

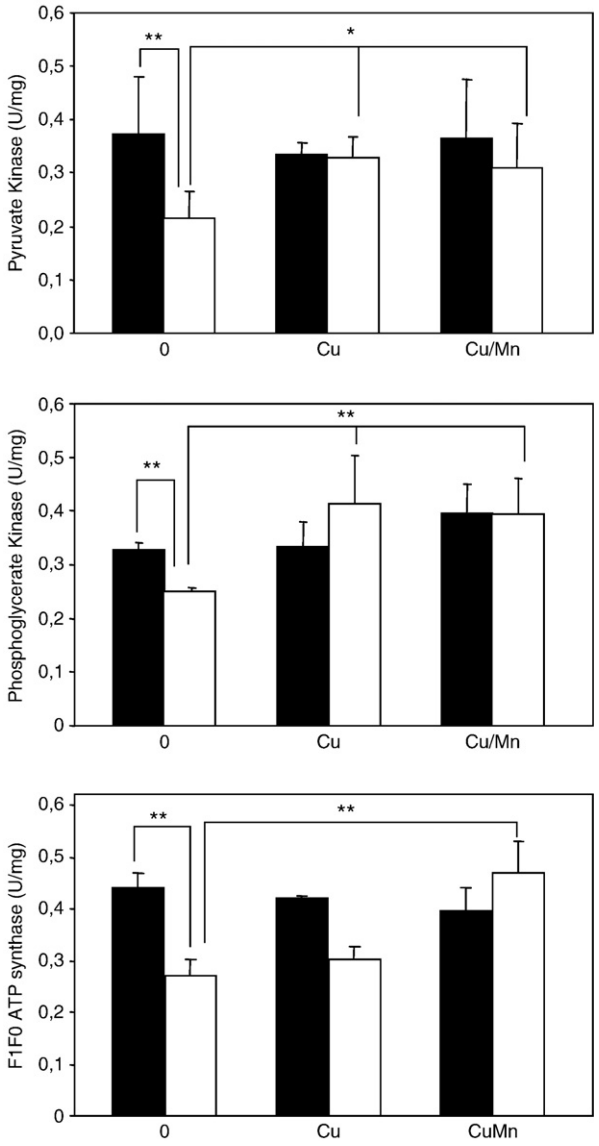

Fig. 4. Recovery of specific activity of carbonylated enzymes in Δ*yfh1* yeast cells by metal treatment. Wild-type (black bars) and Δ*yfh1* cells (white bars) were grown in YPG supplemented with 50 μM $MnCl_2$ and 5 μM $CuSO_4$ as indicated. Control cultures were grown without supplementation. Enzymatic activity of pyruvate kinase and phosphoglycerate kinase was measured in whole-cell extracts. F_1F_0-ATP synthase was measured in mitochondrial preparations from wild-type and Δ*yfh1* cells, and the activity found in Δ*yfh1* mitochondria was corrected according to the relative amount of mitochondrial porin present in each preparation (detected by Western blot). Data are presented as means ± standard deviation from three independent experiments. Combined copper and manganese treatment provided a significant protection of the three enzymatic activities. Copper alone provided significant protection to cytosolic enzymatic activity but failed to protect F_1F_0-ATP synthase (*$P<0.05$, **$P<0.01$).

Cultures of 1 ml containing various concentrations of copper and manganese in YPG were incubated for 18 h in 24-well plates in a Biotek PowerWave XS microplate spectrophotometer. An equal number of cells were inoculated in each well at the beginning of the experiment, and optical density was measured every 30 min. Maximum generation times were calculated for each culture considering at least a 4-h period. Cells lacking Yfh1 presented longer generation times (208 min) than wild-type cells (156 min). Copper or manganese treatment, alone (Fig. 6) or combined (not shown), did not significantly affect these parameters. This fact indicates that the reduced growth rate in Δ*yfh1* cells is not due to increased protein damage to Mg-binding proteins or FeS enzymes recovered by copper and manganese treatment.

We also wanted to test the sensitivity of both strains to the superoxide-generating agent menadione, as well as the effect of metal supplementation on such sensitivity. For this purpose, cell cultures were challenged with 2.5 μM menadione 4 h after metal treatment and growth rate was monitored for 14 additional hours. Maximum generation times were calculated as described. Menadione had a strong effect on Δ*yfh1* generation time (461 min, more than double), but did not have a significant effect on wild-type generation time. Copper and manganese treatments had divergent effects on the increased sensitivity of the Δ*yfh1* strain to menadione. Copper decreased sensitivity but manganese increased it in a dose-dependent manner (Fig. 6). These results confirm that Δ*yfh1* cells are more sensitive to oxidative stress than wild-type cells and suggest that decreased CuZn-SOD activity is involved in such sensitivity. Supporting this idea, experiments carried out with a double mutant, Δ*yfh1*Δ*sod1*, showed that it was unable to grow aerobically (data not shown), which is in accordance with a deleterious effect of decreased SOD activity in cells lacking Yfh1.

Pyruvate kinase activity in Δsod1 cells: effect of copper supplementation

To further investigate the contribution of decreased SOD activity to protein oxidation, we analyzed pyruvate kinase activity in a Δ*sod1* strain. Because this mutant does not grow in YPG, cells were grown in YPD for these experiments. As shown in Fig. 7, pyruvate kinase activity presented a significant decrease in Δ*sod1*, similar to that observed in the Δ*yfh1* mutant grown under the same conditions. Interestingly, in contrast to what was observed in Δ*yfh1* cells, enzymatic activity was not recovered in Δ*sod1* cells grown in copper-supplemented medium. This result indicates that the recovery of pyruvate kinase by copper treatment in Δ*yfh1* cells is due to the recovery of CuZn-SOD activity and not to any other indirect effect exerted by copper treatment.

Both Δyfh1 and Δsod1 strains show increased levels of chelatable iron

Previously, we had shown that chelatable iron was the fraction responsible for protein oxidative damage in Δ*yfh1* cells [15]. A possible link between SOD activity and oxidative damage to proteins could be directly related to the known ability of superoxide to increase the fraction of chelatable iron [29]. To investigate this point, we measured the relative content of chelatable iron in wild-type, Δ*yfh1*, and Δ*sod1* cells grown in YPD, as well as the total cellular iron content after acid digestion of the cells. Chelatable iron can be estimated with the use of Phen Green SK, a cell-permeative fluorescent sensor carrying a phenanthroline group. Inside cells, the fluorescence of this sensor is quenched by iron binding and can be recovered after addition of the cell-permeative iron chelator 1,10-phenanthroline to the cell suspension [30]. Cells were washed with synthetic medium, loaded with 20 μM Phen Green SK diacetate for 20 min, and washed again with synthetic medium and the fluorescence was recorded in a confocal microscope. After basal fluorescence was recorded for 1 min, 2 mM 1,10-phenanthroline was added to the preparation and fluorescence recorded for 4 additional minutes. Figs. 8A–8F shows the images of wild-type Δ*sod1* and Δ*yfh1* cells before and 90 s after the addition of 1,10-phenanthroline. The mean recorded fluorescence for both strains at various times is shown in Fig. 8G. A sharp increase in fluorescence intensity, followed by a plateau, is observed soon after the addition of the chelator. Subtracting the basal fluorescence of each cell from the fluorescence of the same cell after 90 s of exposure to 1,10-phenanthroline yielded the relative amount of chelatable iron (shown in Fig. 8H). This value was obtained from at least 30 cells from three independent experiments. As shown in Fig. 8H, both mutants exhibited increased amounts of chelatable iron. When total cell iron content was measured, Δ*sod1* cells did not show a significant increase in total iron in contrast to what was observed in Δ*yfh1* cells. These results

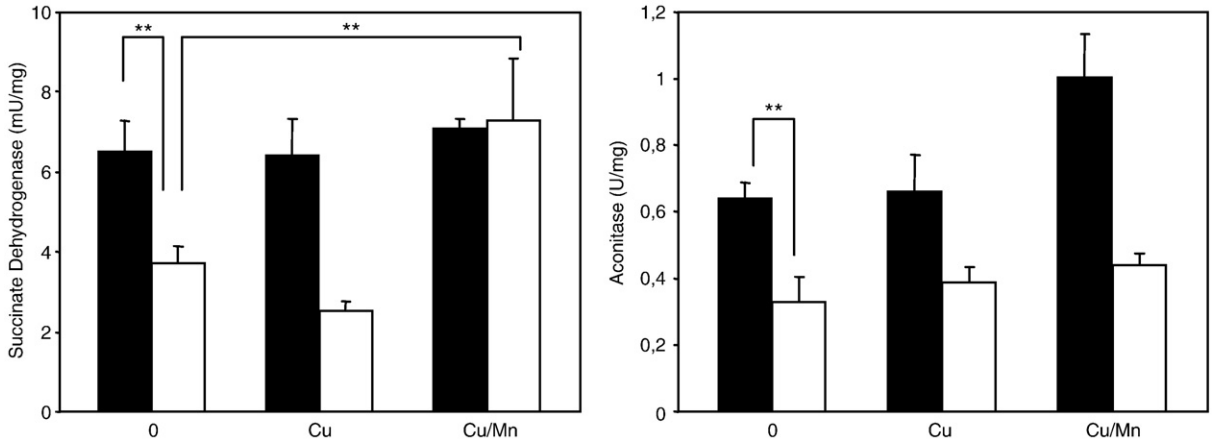

Fig. 5. Specific activity of mitochondrial FeS enzymes in Δ*yfh1* yeast cells is not recovered by copper treatment. Wild-type (black bars) and Δ*yfh1* cells (white bars) were grown in YPG medium supplemented with 50 μM $MnCl_2$ and 5 μM $CuSO_4$ as indicated. Control cultures were grown without supplementation. Enzymatic activity was measured in whole-cell extracts. Data are presented as means ± standard deviation from three independent experiments. Combined copper and manganese treatment provided significant protection of succinate dehydrogenase but not of aconitase. Copper alone did not protect any of these enzymes (**$P<0.01$).

indicate that chelatable iron formation in Δ*yfh1* cells is promoted by decreased SOD activity.

Discussion

In a previous study, we described the presence of high levels of chelatable iron, oxidative damage to Mg-binding proteins, and decreased SOD activity in Δ*yfh1* mutants. This study investigated the role of SOD deficiency in promoting oxidative damage under iron-overload conditions. Our results suggest a central role for both SODs in promoting protein oxidative damage, consistent with previously published observations and represented in Fig. 9. It has been widely described that loss of Yfh1 activates the iron regulon AFT1, which in turn promotes Ftr1 and Fet3 expression and iron acquisition [10,15,26]. Activation of AFT1 leads to copper-deprived cytosol, as this metal is required for the ferroxidase activity of Fet3 [27]. This would result in decreased cytosolic SOD activity, which would promote the inactivation of iron–sulfur enzymes and trigger the formation of chelatable iron. This form of iron would replace Mg from Mg-binding sites and promote the specific damage to Mg-binding proteins [15]. Yfh1 depletion also induces a decrease in manganese uptake, through a still unknown mechanism [16]. This results in decreased Mn-SOD activity, which has effects in mitochondria similar to those exerted by decreased CuZn-SOD activity in the cytosol. Moreover, Mn-SOD may be inactivated by iron [17], leading to a vicious cycle that promotes further increase in superoxide levels and decreased activity of target enzymes. This vicious cycle can be prevented by enhancing the cofactor availability (copper and manganese), allowing partial recovery of both SOD activities and, consequently, preventing the oxidation of most of the enzymes targeted by superoxide. In Δ*sod1* cells, increased superoxide levels

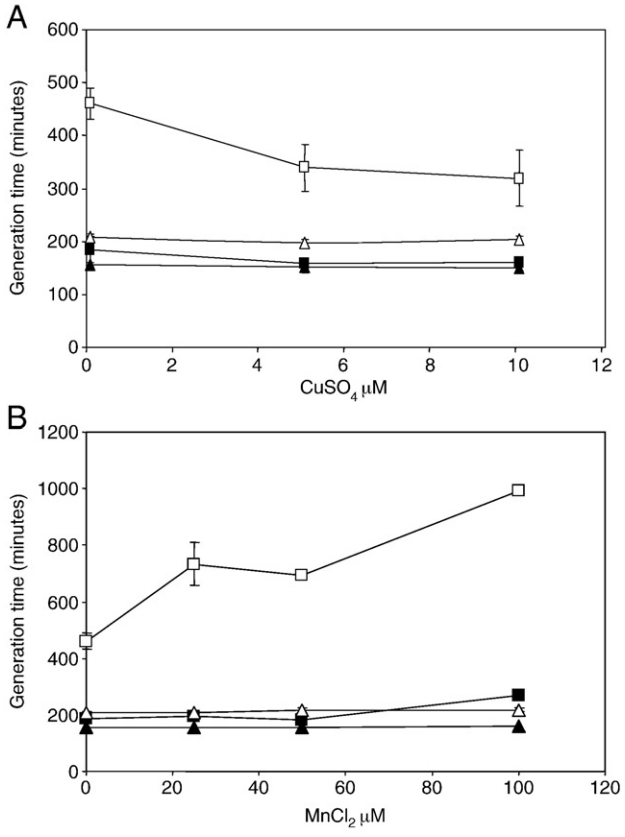

Fig. 6. Effects of menadione, copper, and manganese on the generation time of wild-type and Δ*yfh1* cells. Wild-type (black markers) and Δ*yfh1* cells (white markers) were grown in 24-well plates in YPG medium containing the indicated amounts of (A) $CuSO_4$ or (B) $MnCl_2$ and stressed by 2.5 μM menadione (square markers) or not stressed (triangles). Generation time was calculated for each condition as explained under Experimental procedures. Data are presented as means ± confidence intervals from six independent cultures.

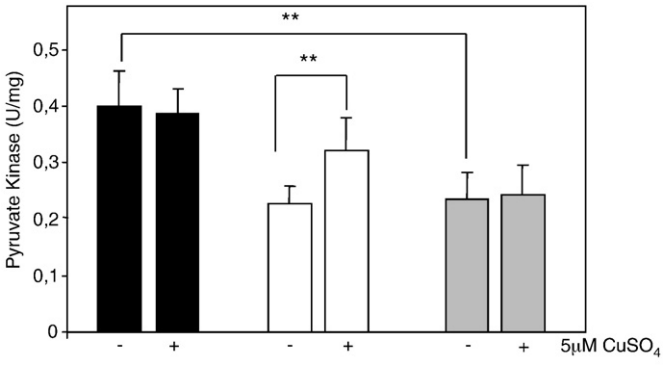

Fig. 7. Effects of copper supplementation on pyruvate kinase activity in Δ*yfh1* and Δ*sod1* cells. Wild-type (black bars), Δ*yfh1* (white bars), and Δ*sod1* (gray bars) cells were grown in YPD medium supplemented with 5 μM $CuSO_4$ or without supplementation and pyruvate kinase activity was measured in whole-cell extracts. Values are U/mg of total protein. Data are presented as means ± standard deviation from three independent experiments. A significant protection in pyruvate kinase activity (**$P<0.01$) was provided by copper treatment in Δ*yfh1* cells but not in Δ*sod1* cells.

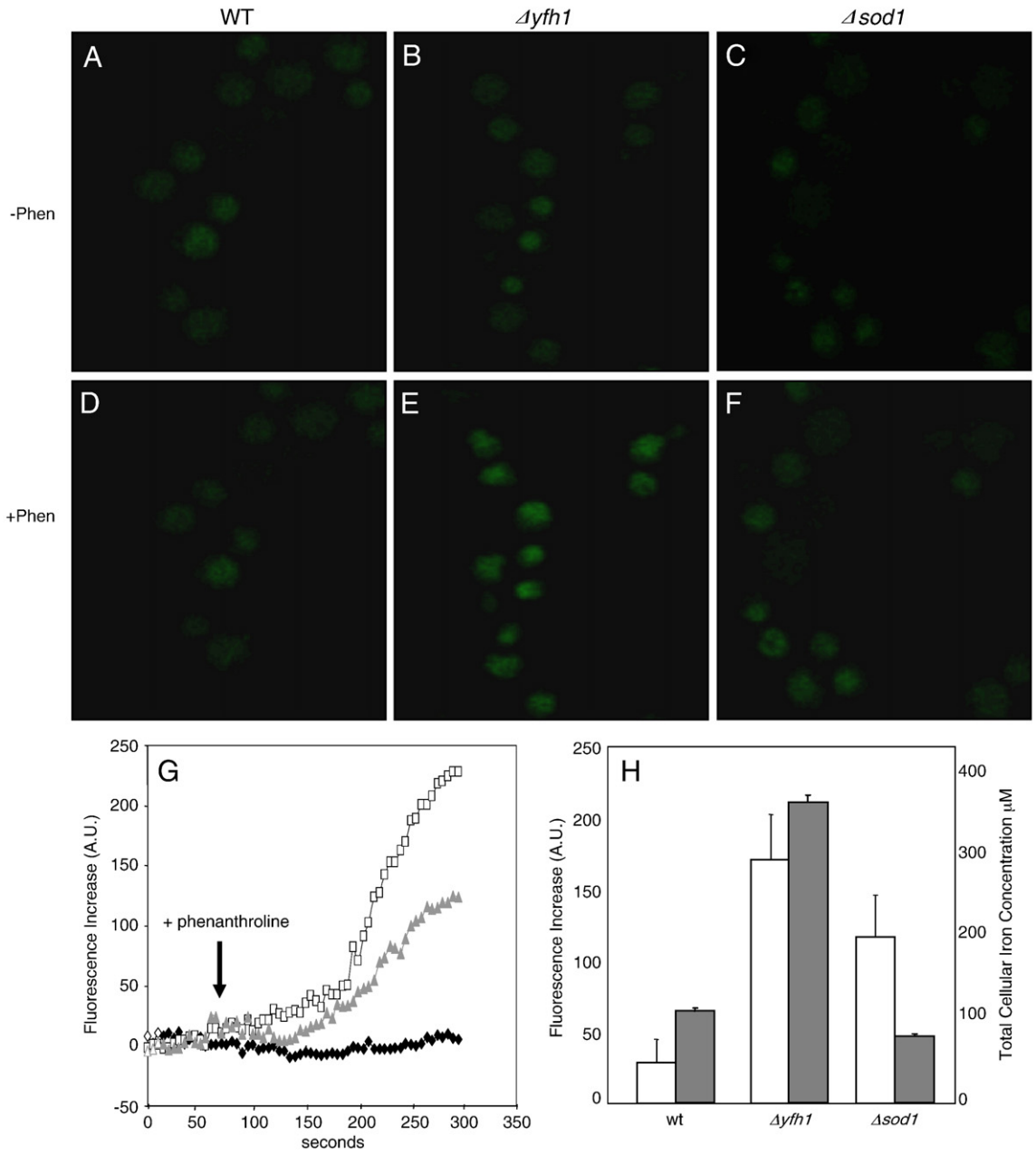

Fig. 8. Increased levels of chelatable iron in Δ*yfh1* cells. Wild-type, Δ*yfh1*, and Δ*sod1* cells were grown in YPD medium, washed with SC medium, and then loaded for 20 min with 20 μM Phen Green SK diacetate. Images were obtained by confocal microscopy using a 505 nm longpass filter ($\lambda_{excitation}$ 488 nm). (A–F) Images collected (A–C) before and (D–F) 90 s after the addition of 1,10-phenantholine to wild-type (A, D), Δ*yfh1* (B, E), and Δ*sod1* cells (C, F). (G) A representative experiment is shown. Each series corresponds to the average fluorescence of 30 cells found in the same microscopic field from wild-type (♦), Δ*yfh1* (□), or Δ*sod1* (▲) strains. Basal fluorescence was recorded for 1 min. An increase in fluorescence was observed after the addition of 2 mM 1,10-phenanthroline to the preparation (arrow). (H) Relative levels of chelatable iron (white bars) and total iron content (gray bars) in the three strains analyzed. To obtain the chelatable iron value, the fluorescence recorded before 1,10-phenanthroline addition was subtracted from that recorded for the same cell 90 s after addition of the chelator. Values for a minimum of 30 cells were recorded in each experiment. Total cell iron was calculated after acid digestion of the cells as described under Experimental procedures. Data are presented as means ± standard deviation from three independent experiments.

due to the absence of cytosolic SOD activity also result in increased chelatable iron and inactivation of Mg-binding enzymes such as pyruvate kinase. However, copper supplementation is not able to restore the SOD activity and, consequently, inactivation of pyruvate kinase is not prevented by this treatment.

Considering all of these elements, then, what is the relevance of SOD deficiency on cellular function or viability? The analysis of the effect of metal supplementation on growth rate indicates that the decreased growth rate of the Δ*yfh1* strain under basal conditions is not due to decreased SOD activity. However, this is not the case when cells are exposed to a slight oxidative challenge such as the addition of 2.5 μM menadione to the culture medium. Under such conditions, copper treatment significantly ameliorates the slow growth rate of Δ*yfh1* cells. This fact indicates that decreased CuZn-SOD activity is directly involved in the increased sensitivity of Yfh1-deficient cells to oxidative stress. In contrast, manganese supplementation has a negative effect on the growth rate of Δ*yfh1* cells in the presence of menadione. It should be considered that menadione toxicity can be mediated by cytosolic enzymes such as glutathione *S*-transferase [32] or cytosolic quinone oxidoreductases [33] acting as reductants of the drug. In this context, restoring Mn-SOD activity would not have any effect under menadione stress. In addition, it is known that manganese has both beneficial and toxic effects [31]; under the conditions tested, the detrimental impact on cell viability

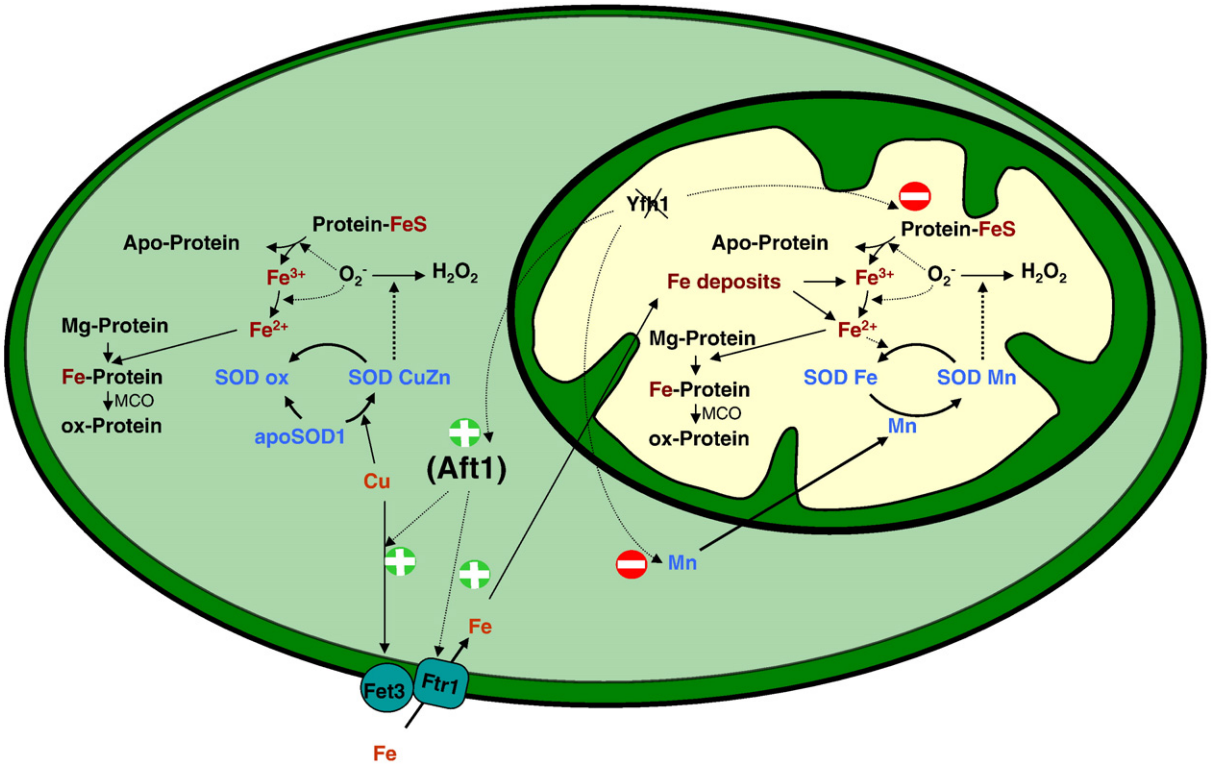

Fig. 9. Proposed mechanism to explain the role of SOD deficiency in promoting oxidative damage under iron-overload conditions. Manganese deficiency in Δ*yfh1* cells was previously described (Ref. [15]) as affecting SOD2 activity. Supplementation of the culture medium with this metal decreases the damage to mitochondrial proteins (this study). Also, AFT1 induction in Δ*yfh1* cells enhances the recruitment of copper by membrane transporters (Ref. [27]) and, as a consequence, SOD1 activity is decreased. Supplementation of the cultures with copper restores normal levels of SOD1 activity and, as a result, the oxidative damage to cytosolic proteins is decreased (this study). For more details, see text.

would be greater than the beneficial effects of restoring Mn-SOD activity. Nevertheless, the increased sensitivity of Yfh1-deficient cells toward menadione should not be considered a minor point because patients suffering Friedreich ataxia or other iron-overloading pathologies may be exposed to many environmental challenges during their lifetime that could compromise cellular function. In this context, any treatment restoring the activity of superoxide dismutases would improve the oxidative stress resilience of cells exposed to iron overload. Indeed, lowered SOD activity could explain the increased sensitivity of frataxin-deficient cells to oxidative stress. Of course, iron overload would trigger the formation of O_2^- or $^{\bullet}OH$ radicals and sensitize frataxin-deficient cells to oxidative stress. It is worth mentioning that alterations in SOD activity and expression have been reported in other FRDA models. Hearts from conditional mouse models of FRDA display decreased total SOD activity [34] and abnormal expression of Mn-SOD [35]. More recently, fibroblasts from FRDA patients were shown to be unable to induce Mn-SOD expression after an oxidative stress challenge [36]. In both cases, however, the contribution of this decreased SOD activity on cellular dysfunction was discussed, because treatment with Mn-TBAP (a compound considered a SOD mimetic) did not exert any beneficial effect in either model. It should be considered, however, that recent reports indicate that this compound would have low O_2^- scavenging activity [37]. To our knowledge, other known SOD mimetics, like some EUK compounds that have proven effective in *sod*$^{-/-}$ mice [38], have not been tested in any frataxin-deficient model. In conditional mouse models of FRDA [35], no positive effects on survival were observed by overexpression of human SOD1. However, negative results in such experiments are not conclusive, as SOD1 overexpression has also been reported to trigger negative effects in mice [39]. Thus, the relevance of decreased SOD activity in the pathophysiology of FRDA remains an open question. In this context, metal treatment could be an alternative approach to increasing SOD activities. However, this approach would require further work in mammalian models of the disease to uncover the mechanisms responsible for SOD deficiency in such models.

Some interesting questions remain unanswered regarding Yfh1 function and the consequences of its absence on metal homeostasis. It is clear that loss of Yfh1 activates AFT1, but the precise mechanism linking both proteins is not completely understood. Yfh1 has been frequently reported to be involved in iron–sulfur biogenesis and disruption of this process is known to activate AFT1 [40]. However, several studies have questioned whether Yfh1 plays an essential role in iron–sulfur biogenesis [16,41–43], and other roles such as iron storage/detoxification [44], electron transfer to ubiquinone [45], or heme biosynthesis [46] have been proposed for frataxin or Yfh1. Any of these roles, in conjunction with a nonessential involvement in iron–sulfur biogenesis or not, could create an imbalance in mitochondrial iron homeostasis that would trigger AFT1 activation. Once AFT1 is activated, increased iron deposits and decreased copper availability could promote SOD deficiency and begin an unending cycle of increased superoxide levels, inactivation of iron–sulfur enzymes, stronger AFT1 activation, and enhanced SOD deficiency. Finally, the intriguing question of the origin of manganese deficiency deserves further investigation to determine whether it is a direct consequence of Yfh1 deficiency or is secondary to AFT1 activation, iron accumulation, or any other consequence of Yfh1 depletion.

Acknowledgments

This work was supported by Grants BFU2004-00593/BMC and CSD2007-00020 from the Ministerio de Ciencia e Innovacion and SGR 0677 from Generalitat de Catalunya (Spain). V.I. received a Ph.D. fellowship from the Generalitat de Catalunya. We thank Elaine M. Lilly for editorial assistance.

References

[1] Fontecave, M.; Pierre, J. L. Iron: metabolism, toxicity and therapy. *Biochimie* **75:** 767–773; 1993.

[2] De Domenico, I.; McVey Ward, D.; Kaplan, J. Regulation of iron acquisition and storage: consequences for iron-linked disorders. *Nat. Rev. Mol. Cell Biol.* **9:**72–81; 2008.

[3] Eaton, J. W.; Qian, M. Molecular bases of cellular iron toxicity. *Free Radic. Biol. Med.* **32:**833–840; 2002.

[4] Toyokuni, S. Role of iron in carcinogenesis: cancer as a ferrotoxic disease. *Cancer Sci.* **100:**9–16; 2009.

[5] Salazar, J.; Mena, N.; Hunot, S.; Prigent, A.; Alvarez-Fischer, D.; Arredondo, M.; Duyckaerts, C.; Sazdovitch, V.; Zhao, L.; Garrick, L. M.; Nuñez, M. T.; Garrick, M. D.; Raisman-Vozari, R.; Hirsch, E. C. Divalent metal transporter 1 (DMT1) contributes to neurodegeneration in animal models of Parkinson's disease. *Proc. Natl. Acad. Sci. USA* **105:**18578–18583; 2008.

[6] Campuzano, V.; Montermini, L.; Molto, M. D.; Pianese, L.; Cossee, M.; Cavalcanti, F.; Monros, E.; Rodius, F.; Duclos, F.; Monticelli, A.; Zara, F.; Canizares, J.; Koutnikova, H.; Bidichandani, S. I.; Gellera, C.; Brice, A.; Trouillas, P.; De Michele, G.; Filla, A.; De Frutos, R.; Palau, F.; Patel, P. I.; Di Donato, S.; Mandel, J. L.; Cocozza, S.; Koenig, M.; Pandolfo, M. Friedreich's ataxia: autosomal recessive disease caused by an intronic GAA triplet repeat expansion. *Science* **271:**1423–1427; 1996.

[7] Boddaert, N.; Le Quan Sang, K. H.; Rotig, A.; Leroy-Willig, A.; Gallet, S.; Brunelle, F.; Sidi, D.; Thalabard, J. C.; Munnich, A.; Cabantchik, Z. I. Selective iron chelation in Friedreich ataxia: biologic and clinical implications. *Blood* **110:**401–408; 2007.

[8] Rotig, A.; Sidi, D.; Munnich, A.; Rustin, P. Molecular insights into Friedreich's ataxia and antioxidant-based therapies. *Trends Mol. Med.* **8:**221–224; 2002.

[9] Rotig, A.; de Lonlay, P.; Chretien, D.; Foury, F.; Koenig, M.; Sidi, D.; Munnich, A.; Rustin, P. Aconitase and mitochondrial iron–sulphur protein deficiency in Friedreich ataxia. *Nat. Genet.* **17:**215–217; 1997.

[10] Babcock, M.; de Silva, D.; Oaks, R.; Davis-Kaplan, S.; Jiralerspong, S.; Montermini, L.; Pandolfo, M.; Kaplan, J. Regulation of mitochondrial iron accumulation by Yfh1p, a putative homolog of frataxin. *Science* **276:**1709–1712; 1997.

[11] Cavadini, P.; Gellera, C.; Patel, P. I.; Isaya, G. Human frataxin maintains mitochondrial iron homeostasis in Saccharomyces cerevisiae. *Hum. Mol. Genet.* **9:**2523–2530; 2000.

[12] Pierre, J. L.; Fontecave, M. Iron and activated oxygen species in biology: the basic chemistry. *Biometals* **12:**195–199; 1999.

[13] Kakhlon, O.; Cabantchik, Z. I. The labile iron pool: characterization, measurement, and participation in cellular processes, 1. *Free Radic. Biol. Med.* **33:**1037–1046; 2002.

[14] Petrat, F.; de Groot, H.; Sustmann, R.; Rauen, U. The chelatable iron pool in living cells: a methodically defined quantity. *Biol. Chem.* **383:**489–502; 2002.

[15] Irazusta, V.; Moreno-Cermeno, A.; Cabiscol, E.; Ros, J.; Tamarit, J. Major targets of iron-induced protein oxidative damage in frataxin-deficient yeasts are magnesium-binding proteins. *Free Radic. Biol. Med.* **44:**1712–1723; 2008.

[16] Irazusta, V.; Cabiscol, E.; Reverter-Branchat, G.; Ros, J.; Tamarit, J. Manganese is the link between frataxin and iron–sulfur deficiency in the yeast model of Friedreich ataxia. *J. Biol. Chem.* **281:**12227–12232; 2006.

[17] Yang, M.; Cobine, P. A.; Molik, S.; Naranuntarat, A.; Lill, R.; Winge, D. R.; Culotta, V. C. The effects of mitochondrial iron homeostasis on cofactor specificity of superoxide dismutase 2. *EMBO J.* **25:**1775–1783; 2006.

[18] Jouihan, H. A.; Cobine, P. A.; Cooksey, R. C.; Hoagland, E. A.; Boudina, S.; Abel, E. D.; Winge, D. R.; McClain, D. A. Iron-mediated inhibition of mitochondrial manganese uptake mediates mitochondrial dysfunction in a mouse model of hemochromatosis. *Mol. Med.* **14:**98–108; 2008.

[19] Rodriguez-Manzaneque, M. T.; Tamarit, J.; Belli, G.; Ros, J.; Herrero, E. Grx5 is a mitochondrial glutaredoxin required for the activity of iron/sulfur enzymes. *Mol. Biol. Cell* **13:**1109–1121; 2002.

[20] Fenton, A. W.; Blair, J. B. Kinetic and allosteric consequences of mutations in the subunit and domain interfaces and the allosteric site of yeast pyruvate kinase. *Arch. Biochem. Biophys.* **397:**28–39; 2002.

[21] Maitra, P. K.; Lobo, Z. A kinetic study of glycolytic enzyme synthesis in yeast. *J. Biol. Chem.* **246:**475–488; 1971.

[22] Mueller, D. M. Arginine 328 of the beta-subunit of the mitochondrial ATPase in yeast is essential for protein stability. *J. Biol. Chem.* **263:**5634–5639; 1988.

[23] Velours, J.; Vaillier, J.; Paumard, P.; Soubannier, V.; Lai-Zhang, J.; Mueller, D. M. Bovine coupling factor 6, with just 14.5% shared identity, replaces subunit h in the yeast ATP synthase. *J. Biol. Chem.* **276:**8602–8607; 2001.

[24] Manchenko, G. P. Handbook of Detection of Enzymes on Electrophoretic Gels. CRC Press, Boca Raton, FL; 1994.

[25] Tamarit, J.; Irazusta, V.; Moreno-Cermeno, A.; Ros, J. Colorimetric assay for the quantitation of iron in yeast. *Anal. Biochem.* **351:**149–151; 2006.

[26] Foury, F.; Talibi, D. Mitochondrial control of iron homeostasis: a genome wide analysis of gene expression in a yeast frataxin-deficient strain. *J. Biol. Chem.* **276:** 7762–7768; 2001.

[27] Philpott, C. C.; Protchenko, O. Response to iron deprivation in Saccharomyces cerevisiae. *Eukaryotic Cell* **7:**20–27; 2007.

[28] Wallace, M. A.; Liou, L. L.; Martins, J.; Clement, M. H.; Bailey, S.; Longo, V. D.; Valentine, J. S.; Gralla, E. B. Superoxide inhibits 4Fe–4S cluster enzymes involved in amino acid biosynthesis: cross-compartment protection by CuZn-superoxide dismutase. *J. Biol. Chem.* **279:**32055–32062; 2004.

[29] Srinivasan, C.; Liba, A.; Imlay, J. A.; Valentine, J. S.; Gralla, E. B. Yeast lacking superoxide dismutase(s) show elevated levels of "free iron" as measured by whole cell electron paramagnetic resonance. *J. Biol. Chem.* **275:**29187–29192; 2000.

[30] Petrat, F.; de Groot, H.; Rauen, U. Subcellular distribution of chelatable iron: a laser scanning microscopic study in isolated hepatocytes and liver endothelial cells. *Biochem. J.* **356:**61–69; 2001.

[31] Gunter, T. E.; Gavin, C. E.; Aschner, M.; Gunter, K. K. Speciation of manganese in cells and mitochondria: a search for the proximal cause of manganese neurotoxicity. *Neurotoxicology* **27:**765–776; 2006.

[32] Zadzinski, R.; Fortuniak, A.; Bilinski, T.; Grey, M.; Bartosz, G. Menadione toxicity in Saccharomyces cerevisiae cells: activation by conjugation with glutathione. *Biochem. Mol. Biol. Int.* **44:**747–759; 1998.

[33] Long 2nd, D. J.; Iskander, K.; Gaikwad, A.; Arin, M.; Roop, D. R.; Knox, R.; Barrios, R.; Jaiswal, A. K. Disruption of dihydronicotinamide riboside:quinone oxidoreductase 2 (NQO2) leads to myeloid hyperplasia of bone marrow and decreased sensitivity to menadione toxicity. *J. Biol. Chem.* **277:**46131–46139; 2002.

[34] Chantrel-Groussard, K.; Geromel, V.; Puccio, H.; Koenig, M.; Munnich, A.; Rotig, A.; Rustin, P. Disabled early recruitment of antioxidant defenses in Friedreich's ataxia. *Hum. Mol. Genet.* **10:**2061–2067; 2001.

[35] Seznec, H.; Simon, D.; Bouton, C.; Reutenauer, L.; Hertzog, A.; Golik, P.; Procaccio, V.; Patel, M.; Drapier, J. C.; Koenig, M.; Puccio, H. Friedreich ataxia: the oxidative stress paradox. *Hum. Mol. Genet.* **14:**463–474; 2005.

[36] Paupe, V.; Dassa, E. P.; Goncalves, S.; Auchere, F.; Lonn, M.; Holmgren, A.; Rustin, P. Impaired nuclear Nrf2 translocation undermines the oxidative stress response in Friedreich ataxia. *PLoS One* **4:**e4253; 2009.

[37] Batinic-Haberle, I.; Cuzzocrea, S.; Reboucas, J. S.; Ferrer-Sueta, G.; Mazzon, E.; Di Paola, R.; Radi, R.; Spasojevic, I.; Benov, L.; Salvemini, D. Pure MnTBAP selectively scavenges peroxynitrite over superoxide: comparison of pure and commercial MnTBAP samples to MnTE-2-PyP in two models of oxidative stress injury, an SOD-specific Escherichia coli model and carrageenan-induced pleurisy. *Free Radic. Biol. Med.* **46:**192–201; 2009.

[38] Melov, S.; Doctrow, S. R.; Schneider, J. A.; Haberson, J.; Patel, M.; Coskun, P. E.; Huffman, K.; Wallace, D. C.; Malfroy, B. Lifespan extension and rescue of spongiform encephalopathy in superoxide dismutase 2 nullizygous mice treated with superoxide dismutase-catalase mimetics. *J. Neurosci.* **21:**8348–8353; 2001.

[39] Peled-Kamar, M.; Lotem, J.; Wirguin, I.; Weiner, L.; Hermalin, A.; Groner, Y. Oxidative stress mediates impairment of muscle function in transgenic mice with elevated level of wild-type Cu/Zn superoxide dismutase. *Proc. Natl. Acad. Sci. USA* **94:**3883–3887; 1997.

[40] Hausmann, A.; Samans, B.; Lill, R.; Muhlenhoff, U. Cellular and mitochondrial remodeling upon defects in iron–sulfur protein biogenesis. *J. Biol. Chem.* **283:** 8318–8330; 2008.

[41] Ding, H.; Yang, J.; Coleman, L. C.; Yeung, S. Distinct iron binding property of two putative iron donors for the iron–sulfur cluster assembly: IscA and the bacterial frataxin ortholog CyaY under physiological and oxidative stress conditions. *J. Biol. Chem.* **282:**7997–8004; 2007.

[42] Campanella, A.; Rovelli, E.; Santambrogio, P.; Cozzi, A.; Taroni, F.; Levi, S. Mitochondrial ferritin limits oxidative damage regulating mitochondrial iron availability: hypothesis for a protective role in Friedreich ataxia. *Hum. Mol. Genet.* **18:**1–11; 2008.

[43] Adinolfi, S.; Iannuzzi, C.; Prischi, F.; Pastore, C.; Iametti, S.; Martin, S. R.; Bonomi, F.; Pastore, A. Bacterial frataxin CyaY is the gatekeeper of iron–sulfur cluster formation catalyzed by IscS. *Nat. Struct. Mol. Biol.* **16:**390–396; 2009.

[44] Schagerlof, U.; Elmlund, H.; Gakh, O.; Nordlund, G.; Hebert, H.; Lindahl, M.; Isaya, G.; Al-Karadaghi, S. Structural basis of the iron storage function of frataxin from single-particle reconstruction of the iron-loaded oligomer. *Biochemistry* **47:** 4948–4954; 2008.

[45] Gonzalez-Cabo, P.; Vazquez-Manrique, R. P.; Garcia-Gimeno, M. A.; Sanz, P.; Palau, F. Frataxin interacts functionally with mitochondrial electron transport chain proteins. *Hum. Mol. Genet.* **14:**2091–2098; 2005.

[46] Bencze, K. Z.; Yoon, T.; Millan-Pacheco, C.; Bradley, P. B.; Pastor, N.; Cowan, J. A.; Stemmler, T. L. Human frataxin: iron and ferrochelatase binding surface. *Chem. Commun. (Cambridge)*1798–1800; 2007.